Structure-Thermolysis Relationships for Energetic Materials*

Thomas B. Brill

Department of Chemistry, University of Delaware
Newark, DE 19716, USA

ABSTRACT

The technique of fast thermolysis/FTIR spectroscopy, in which temperature profiling of the condensed phase is also conducted, is described. Applications are given to show how the formation of NO_2, $HONO$, NO, and CH_2O can be related to underlying parent molecular features. The effect of pressure in the 1-1000 psi range on the overall process is presented along with an example of how pressure can be used to distinguish the gas phase reactions from the condensed phase reactions during fast thermolysis.

1. INTRODUCTION

The physicochemical events that take place during the fast thermal decomposition and pre-ignition of energetic materials are among the more poorly understood molecular aspects of the propulsion and explosion process. This is partly because it is extremely difficult to gather information about this regime under realistic conditions. Figure 1 shows a very simple, generalised, one-dimensional view of the main zones. The approximately 100 μm thick region that constitutes endothermic breakup of large molecules to form smaller species that go on to feed the exothermic decomposition flame has been of greatest interest. The overall process of combustion is extremely complicated when one blends details of this thin zone with the detailed chemistry of the gas phase and the fluid mechanics of turbulent diffusion.

20 - 200 μM

OX

FUEL

PREMIXED FLAME

DIFFUSION FLAME
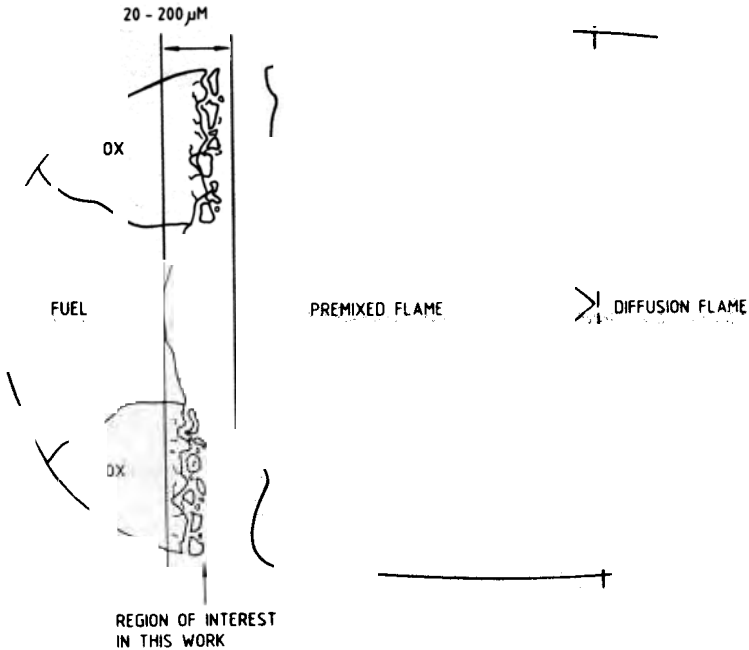
OX

REGION OF INTEREST
IN THIS WORK

Figure 1 A diagram of the region of interest in this research effort.

Given the thinness and complexity of the interface between the condensed phase and near surface gas region, there are no ideal methods to probe the chemistry directly. At present, one must resort to experiments that simulate some or all of the conditions of combustion or explosion. The most relevant experiments employ rapid heating, realistic pressures, and allow gases, liquids and solids to be present simultaneously. Real-time diagnostics are needed because the processes take place dynamically. If such simulation experiments are successful, there are major practical advances possible toward understanding the pre-ignition and ignition of solids, and, at least parts of the combustion process of energetic materials. The enormous complexity of the chemistry and physics mitigate against attempting to specify the events quantitatively at this time. In most cases, even a qualitative phenomenological description is valuable because this level of chemical understanding is frequently not even available from experiment.

Toward filling these voids, we have developed several fast thermolysis/Fourier transform infrared (FTIR) spectroscopy techniques that permit near real-time studies of energetic materials heated at 70-400 °C/s under selected pressures in the 1-1000 psi range.

There are a number of objectives for this research effort. The following subjects are addressed in this paper. First. it was sought to discover structure/property/ decomposition correlations that connect the parent molecular structure and

composition to the evolved gases near the surface. This is a step towards coupling the formulation of the material to its combustion and explosion characteristics. Second, since pressure is such a ubiquitous variable, it was necessary to uncover the effect of pressure on the overall processes. Third, we have been interested in using pressure to probe certain chemical processes.

2. EXPERIMENTAL DESIGN

To achieve the goal, a fast thermolysis cell[1,2] was developed and its principles of operation[1] were described and updated[3]. Figure 2 gives the essential design features of the cell. The anti-reflection coated 0.5″ × 1″ diameter *ZnSe* windows are held in a 3″ diameter aluminium cylinder by brass end caps. *ZnSe* was used because it has good mid-IR throughout and has a high bursting pressure. The cell was designed to withstand a static pressure of 5000 psi, but is used only in the 1-1000 psi range. The filament is a creased nichrome-IV ribbon (2.5 × 0.6 × 0.012 cm) supported on pressure-tight feed through insulators. Typically, 1-2 mg of sample (solid, liquid or mixture) was heated using a Foxboro 40 Pyrochem controller. The constant voltage-variable current features of the controller has special value in the temperature profiling experiments
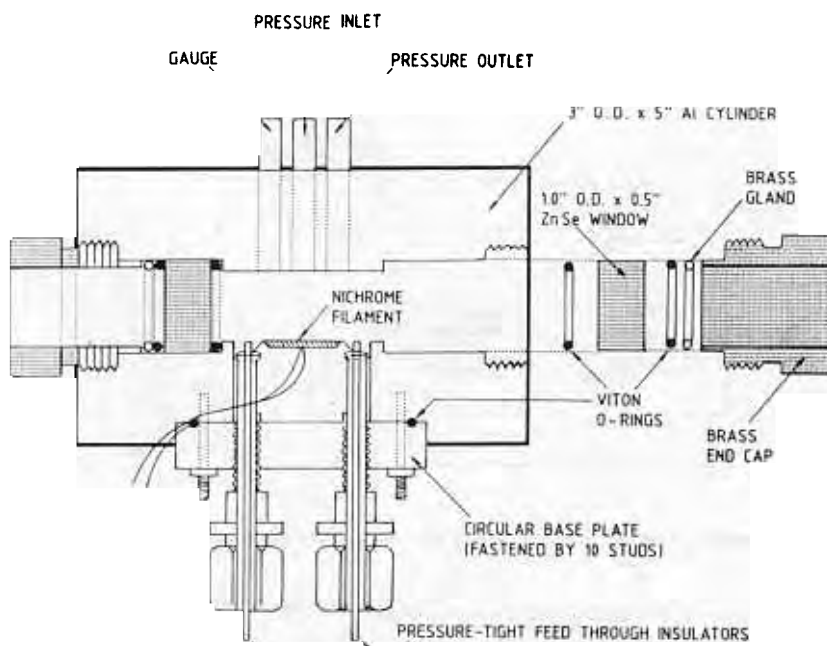

Figure 2.   Essential features of the thermolysis cell.

discussed in the following paragraphs. In principle, any reasonable heating rate of the sample could be achieved, but <400 °C/s was chosen because the spectral collection rate does not distinguish processes at higher heating rates. True combustion heating rates are thousands of degrees per second. The argon gas pressure in the cell was adjusted as desired in the 1-1000 psi range. Because of the importance of collecting IR spectra at high temporal resolution, the rapid-scan mode of a Nicolet 60SX FTIR spectrometer was used in all of these studies. With the beam focused several millimeters above the filament surface, the IR active gas products from the fast heated sample can be detected in near real-time.

It was found that positioning a type-E thermocouple on the underside of the filament opposite the sample and leaving it in place during the thermolysis experiment enabled the endothermic and exothermic events of the condensed phase to be tracked simultaneously with detection of the gas products. This led to the temperature profiling/FTIR techique[2]. It proved to be straightforward to develop this technique because the heating of the filament is achieved by constant voltage-variable current control. Figure 3 shows a block diagram of the circuit used for this temperature profiling experiment. The 60 Hz noise on the filament was removed by a low-pass filter, and the signal amplified by about 100X with a differential amplifier. The analog output was processed through a Metrabyte DAS-16 AD convertor to an IBM-PC. The 'take data' cycle of the interferometer triggered the heating of the filament so that there is a direct correlation between the time, temperature and interferogram. Four hundred data points were collected in the ten-second temperature measurement.
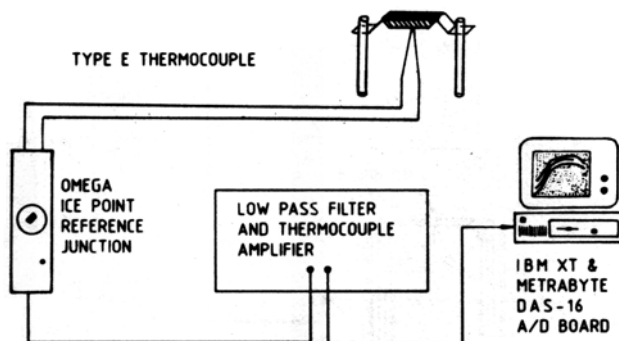

Figure 3.   Thermal analysis part of the temperature profiling/FTIR technique.

In the above experiment, there is no significant time delay between thermolysis and the detection of the evolved gases because the gases need to diffuse several millimeters from the sample to reach the IR beam. The gases rise into the cool *Ar* atmosphere of the cell where they are momentarily quenched during the detection stage. Based on the relative intensities of the *P* and *R* branches, the gases are in their

ground state by the time they reach the IR beam. Argon was used as the atmosphere so that the intrinsic thermolysis characteristics of the parent compound are measured. If, for example, the thermolysis is performed in air, then the intrinsic thermolysis is intermixed with the reactions with O_2 and H_2O.
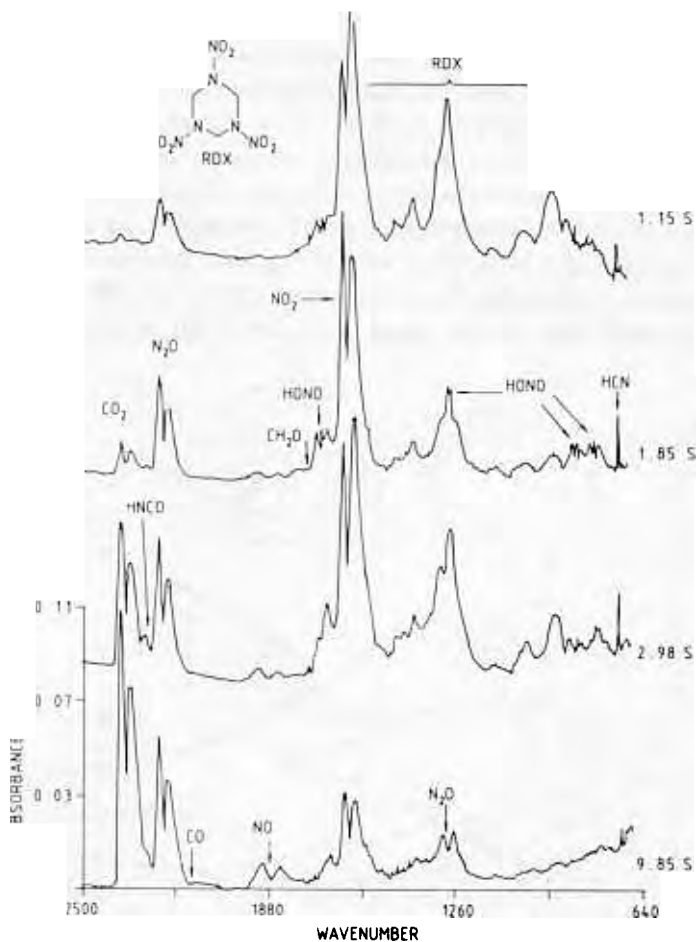

Figure 4. Selected absorbance IR spectra taken 2 mm above the surface of RDX heated at 170 °C/s under 15 psi *Ar*.

Figure 4 illustrates, for a sample of RDX, the good quality spectra that can be obtained. When heated at $dT/dt \simeq 170$ °C/s from room temperature, the initial gases from RDX are first detected in about 1.15 s because the thermal decomposition occurs at about 200 °C. By using the IR intensities, it is possible to convert the observed absorbances to relative per cent concentrations for the IR active gases[1]. Figure 4 shows

relative concentration versus time profiles for RDX. In effect, these are concentrations based on volume. H_2O, IR inactive molecules, and any species for which the IR intensities are unknown (i.e., $HNCO$) are not included. The importance of near real-time analysis of the gas products in fast thermolysis research is evident from Fig. 5. NO_2 is the dominant early decomposition product of RDX, but because of secondary redox reactions, decreases rapidly in concentration, while the concentration of NO increases. It can be noted that NO is negligible at the onset of decomposition. As a result, if the time delay between the analysis and the onset of thermolysis were to exceed five seconds, then different and potentially incorrect conclusions about the thermal decomposition process of RDX could be drawn. The changes in the gas concentrations with time give an indication of secondary reactions among the gases, while the initial gas concentrations are most closely related to the thermolysis of the parent molecule. Based on extensive studies of the thermolysis of nitramines in various reactive atmospheres, the evidence is very strong that the processes leading to the initial gas products occur in the condensed phase[4] Thus, condensed phase processes are largely separated from any gas phase processes in this experiment.
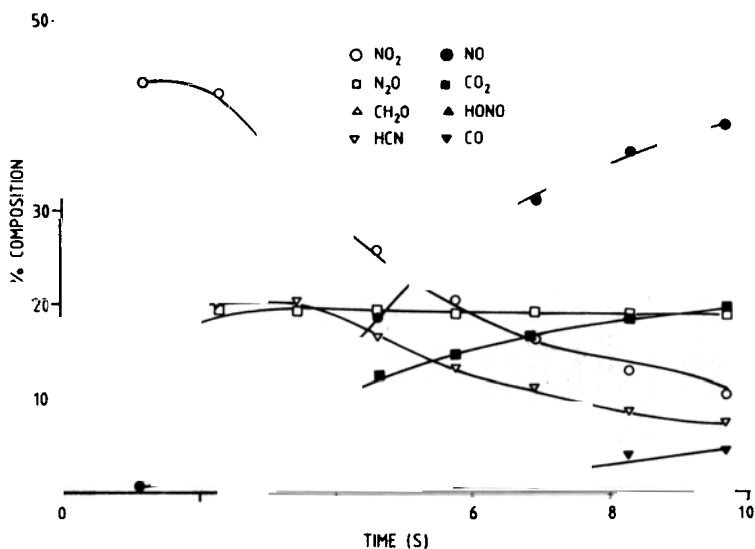

Figure 5. The relative per cent concentrations of the quantified gas products from the spectra shown in Fig. 3.

3. CORRELATIONS OF THE FIRST DETECTED GASES WITH STRUCTURE AND COMPOSITION OF THE PARENT MOLECULE

A determined effort has been made through these fast thermolysis studies to establish the relationships between the structure and composition of the parent

energetic molecules and the near surface gases. These gases dominate the pre-ignition and ignition chemistry of the gas phase. In turn, their products control the flame chemistry. If such connections can be uncovered, then the work of the synthetic chemist could be guided by the combustion and explosives scientist.

Aspects of the parent molecule leading to the formation of the following oxidiser/fuel gases have been uncovered: $NO_2^{5,6}$, $HONO^7$, NO^7, CH_2O^8 and NH_3^9. An overview of the findings are presented here.

3.1 Tendency to form NO_2 (g)

The formation of NO_2 is of major importance in nitramine combustion because it is an oxidiser in the primary flame. Although not discussed earlier as such, it seemed plausible to us that the length of the *N-N* bond in secondary nitramines might be an important factor in the tendency of the *N-N* bond to homolyse and liberate NO_2 upon fast thermolysis. Because of the reactivity of NO_2, it is necessary to draw these conclusions from rapidly heated samples and to employ near real-time detection (IR spectra recorded at 50-100 ms intervals) of the initial gas products. Otherwise, secondary reactions of NO_2 disguise any relationships between its concentration and the structure of the parent molecule. Of course, it must be emphasised that even the simple homolysis of the *N-N* bond in the condensed phase is, overall, a complicated process. Biomolecular activity is possibly present. At the very least, the NO_2 must diffuse through and desorb from the herterogenous environment before it is detected. The most severed complication would be for *N-N* bond homolysis to follow or to compete with another decomposition route, such that the initial *N-N* bond distance would no longer be the controlling factor. If this were the case, then any general structure-decomposition relationship involving NO_2 could be futilely disguised. It was chosen to look for general patterns rather than absolute quantification in this work.

The crystal structures of many nitramines needed to be determined and combined with the structures already available to build the database for this comparison. Putting these together, Fig. 6[5,6] shows a plot of the average *N-N* bond distance versus the average asymmetric NO_2 stretching frequency from the infrared spectrum of a series of secondary nitramines, R_2NNO_2. The compound identities are given elsewhere[5,6]. A reasonably good trend exists between these two parameters suggesting that the force constant of $-NO_2$ stretching depends markedly on the amount of electron density that $-NO_2$ shares with the adjacent *N-N* bond. From fast thermolysis it was found that NO_2 is the dominant, initially detected product for compounds on the right side of this plot. NO_2 was not detected as a lesser abundant product from compounds on the left side. Thus, long *N-N* bonds favour *N-N* scission. Hence, with reasonable confidence one can predict th amount of NO_2 likely to be generated by fast thermolysis of a given secondary nitramine compound from its IR spectrum or crystal structure.

The simple connection in Fig. 6 could be expected to, and does, have exceptions. Several potential causes were mentioned above. Most thermal decomposition processes of complex molecules are a balance of competitive reactions[9]. For instance, a different

degree of stability of the backbone could shift the balance from one mechanism to another[8]. If the backbone is especially stable, as would be expected of the five membered 1,3-dinitroimidizolidine (DNCP) ring, then the rate of ring opening would be slowed relative to N–NO_2 homolysis. This could cause NO_2 to be a major product despite the relatively short N-N bond. This is what is observed for DNCP[7]. NO_2 (and *HONO*) are among the dominant, initially detected gas products even though the N-N bond distance is 1.35 Å. Conversely, a compound with a relatively long N–NO_2 bond distance might produce much less NO_2 than Fig. 6 suggests if the backbone is especially unstable. This is because the decomposition rate might be controlled by the backbone fission route causing the N–NO_2 bond to break more slowly or to be retained in favour of N_2O generation. 1,4-dinitroglycoluril (DINGU)[10] illustrates this behaviour. The average N–NO_2 bond distance is 1.375 Å and v_{as} (NO_2) is 1565 cm^{-1} suggesting that NO_2 should be a significant product. NO_2 is not detected under 15 psi *Ar*, but instead, N_2O dominates. This departure from expectation is attributed to the fact that the backbone is thermally unstable toward the loss of stable products, such as *HONO*, and that the N-N bond is preferentially retained in the fragmentation process of the backbone.
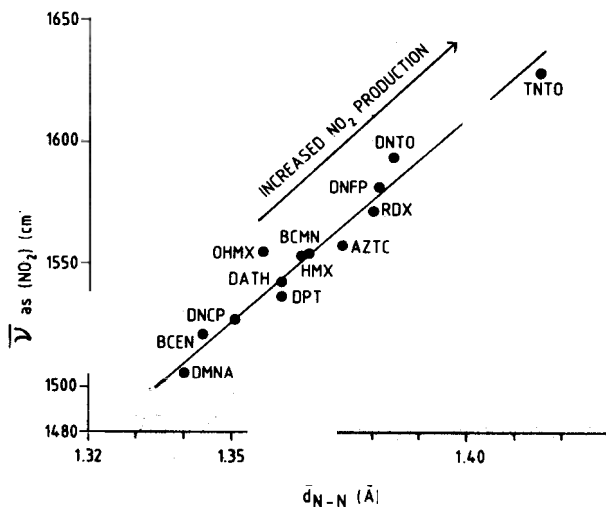

Figure 6. The average asymmetric NO_2 stretching frequency compared to the average N-N bond distance for a series of secondary nitramines.

Despite some exceptions that can be qualitatively rationalised on the basis of competitive or separately preferred decomposition pathways, the fact that most secondary nitramines thermolise in the condensed phase in a systematically predictable way is encouraging. Thermal reactions in the near condensed phase are complex, but

the result above gives hope for uncovering and refining patterns that can be applied in practice to propellant combustion and explosives.

3.2 Tendency to form *HONO* (g)

Closely related to NO_2 is the formation of *HONO*. At least one additional process, that of *H•* participation, is required before *HONO*(g) is detected. The formation of *HONO* has been used in many previous studies of nitramines to rationalise products, but it was not detected directly before fast thermolysis/FTIR spectroscopy was applied. *HONO* is a reactive and, thus, transient molecule which is not observed without rapid heating and near real-time product detection. However, both the *cis-* and *trans-HONO* isomers can now be routinely observed from nitramines[7].
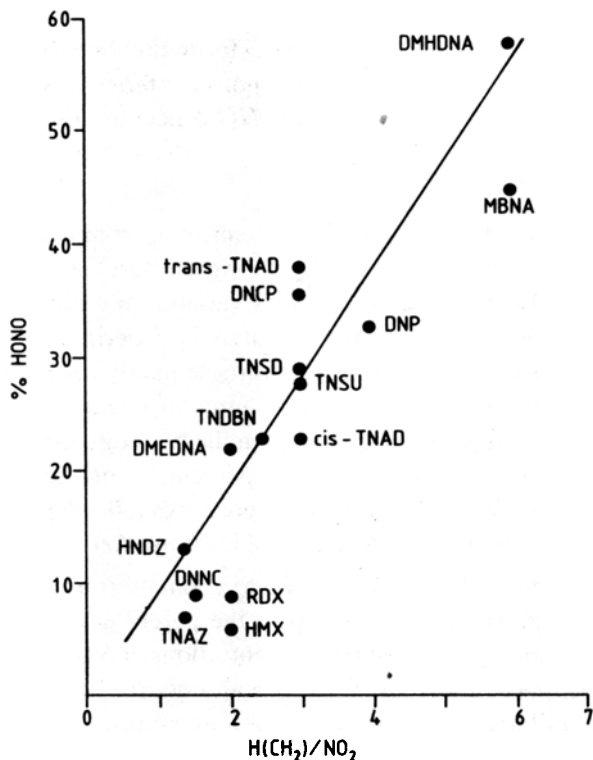

Figure 7. The relative per cent of *HONO* in the first detected gas as a function of the H/NO_2 ratio in the parent molecule.

After examining a large number of nitramines heated at 145-180 °C/s under 15 psi *Ar*, it was discovered that the initial relative per cent concentration of *HONO* depended strongly on the parent secondary nitramine[7]. In one instance, *HONO*

represented nearly 60 per cent of the first detected gas products. A broad relationship was discovered between the ratio of the H atoms to NO_2 groups in the parent molecule and the initial percentage of *HONO* detected is shown in Fig. 7. Insight into the processes by which *HONO* is formed from the condensed phase is contained in the pattern of Fig. 7. The concentration of *HONO* must depend on the adventitious encounter of $H\bullet$ (or an $H\bullet$ source) and $NO_2\bullet$ (or an $NO_2\bullet$ source) in the condensed phase. Statistically, increasing the chance for contact enhances the *HONO* concentration. The molecularity, the nature of the transition state and any other aspects of the reaction mechanism are beyond the extension of these condensed phase data. However, it does not appear that the four- and five-centre concerted reactions that could be important in the gas phase[11], dominate in the condensed phase. If they did, only a $-CH_2-$ fragment adjacent to the nitramine would be required to produce *HONO*. All nitramines having this linkage should produce the same amount of *HONO*, which they do not.

The most plausible explanation for *HONO* formation remains the chance contact between $H\bullet$ and $NO_2\bullet$. In keeping with this notion, steric crowding of H and NO_2 groups in a molecule enhances the initial *HONO* concentration[7].

3.3 Tendency to form *NO(g)*

NO plays a role in the secondary flame chemistry of compounds containing NO_2 groups[12]. It is very rare not to detect *NO* during the fast thermolysis of secondary nitramines. The initial concentration of *NO* is variable, but almost always increases during the ten seconds over which the thermolysis experiment is performed. The relative concentrations of NO_2 and *HONO* decrease nearly monotonically as the *NO* increases. This pattern implies that a major source of *NO* is secondary reactions of NO_2 and *HONO* in the gas phase or, possibly, in the heterogeneous condensed phase. In keeping with this, *NO* becomes a higher percentage of the total gas when the thermolysis is performed at super-atmospheric pressures (30-300 psi), but at a pressure below the range where N_2 usually dominates (>500 psi Ar).

Because the majority of the *NO* appears to emanate from later stage reactions, especially in the gas phase, its relationship to the parent molecular structure in the condensed phase is primarily through the concentrations of NO_2 and *HONO* produced in the primary decomposition steps. First, a major source of *NO* is the equilibrium as shown in Eqn. (1) which favours *NO* at higher temperature. Thus, the concentration of NO_2 should decrease and the concentration of *NO* should increase with the increasing temperature, which they are always found to do in this work. Second, a source of *NO* is the decomposition of *HONO* by reaction shown in Eqn.(2).

$$2NO_2 \quad \longleftrightarrow \quad 2NO + O_2 \qquad\qquad (1$$

$$2HONO \longleftrightarrow NO + NO_2 + H_2O \qquad\qquad (2)$$
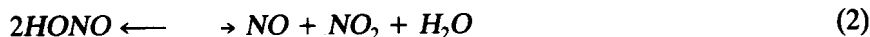
This reaction can account for the high initial abundance of *NO* found when the initial HONO concentration is also high[7]. Third, some nitramines studied also contain aliphatic *C-NO₂* groups. *C-NO₂* compounds are found to generate a considerable amount of $NO^{13,14}$ perhaps because of the approximately thermally neutral *C-NO₂* to *C-ONO* isomerisation[15]. *CO-NO* homolysis leading to *NO* is facile in this isomerised state. Fourth, there is evidence that nitramines can form nitrosamines (*R₂N-NO*) upon thermal decomposition in the condensed phase[16-18]. Fast thermal decomposition of nitrosamines also liberates NO^{19}.

3.4 Tendency to form *CH₂O(g)*

Formaldehyde is an important fuel in the primary flame of nitramines. Most nitramines that liberate *CH₂O* have a –*CH₂*– group straddled by two nitramine groups. There are exceptions to this notion, but it is usually followed. If this unit is usually required in the molecule to assure the formation of *CH₂O*, then it is of interest to learn how the >*NCH₂CH₂N*< unit behaves in a nitramine molecule. This unit is present in many nitramines that we have studied. Ethylene straddled by two nitrogen atoms does not lead to $CH_2O^{8,20}$. When *C-N* bond homolysis occurs in this fragment, the *C-C* bond probably strengthens so that *CH₂O* is not produced. No products containing a *C-C* bond were detected perhaps because *NO₂* oxidised any olefins present.

3.5 Gas Product Predictions Based on Structure/Property/Decomposition Relationships

The relationships described above have qualitative predictive value for anticipating the thermal decomposition characteristics of imagined or newly synthesised energetic nitramines. This point will be illustrated with a new energetic molecule, TDCD. Table 1 lists some observations (causes) for the TDCD molecule and the resulting predictions (effects) about the decomposition gases from fast thermolysis based on these predictions.

Table 1. Observations and predictions about TDCD thermolysis

Cause	Effect
$v_{as}(NO_2) = 1590$ cm	Much *NO₂* generated, therefore much *HCN*, *HNCO*, and *NO* grows as *NO₂* is lost
Few *H* atoms (only ≡ *C-H*)	No *HONO*
No –*CH₂*– straddled by *N*	No *CH₂O*, and no *N₂O*

As shown in Fig. 8, the qualitative predictions in Table 1 about the decomposition gases are borne out well in experiment when TDCD is heated at 110 °C/s under 15 psi Ar^{21}. *NO₂* is indeed the dominant, initially detected product and no *HONO*

is formed. The high initial concentration of NO_2 leads to increased NO formation with time. $HNCO$ (not quantified because its IR intensities are unknown) and HCN are major products. It can be noted that after N-N bond homolysis, the NCO radical and HCN are already set up by connectivity in the backbone to split out. Neither N_2O nor CH_2O are produced.
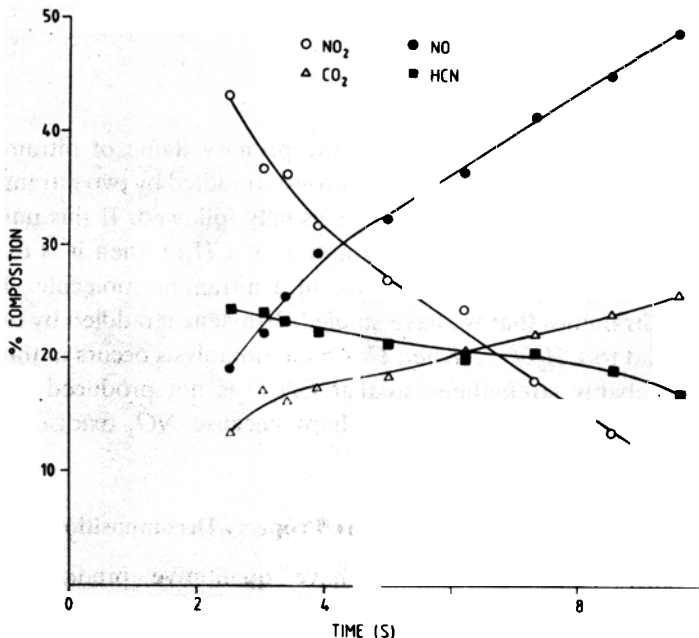

Figure 8. The concentration versus time profile for TDCD heated at 100 °C/s under 15 psi *Ar*.
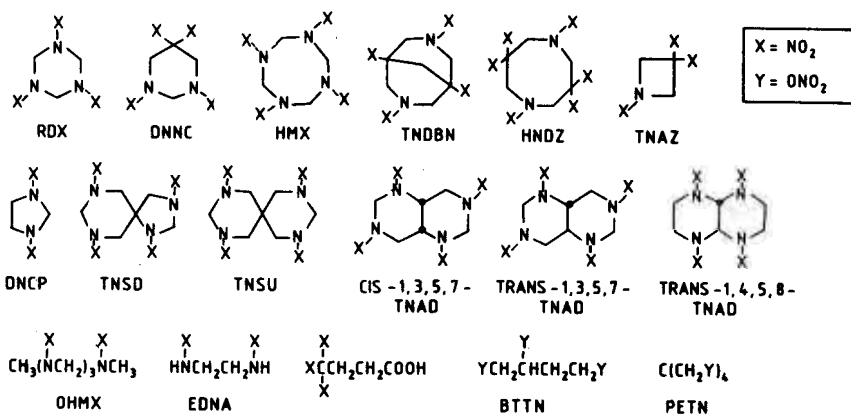
Admittedly, the structure/property/decomposition relationships described above for nitramines do not always give as reliable a prediction as they do for TDCD, but they frequently work well for many products. As mentioned already, discrepancies arise when other reaction pathways compete with or override the one on which the structure/decomposition relationship is based. The central point is that structure/property/decomposition relationships can be uncovered for any class of energetic materials if and when one particular reaction pathway dominates over the others. Competitive reactions, or the occasionally unique and obscure reaction pathway, can lead to a breakdown in the prediction.

4. THE EFFECT OF PRESSURE ON THE FIRST DETECTED PRODUCTS

Pressure is such an important variable in propellant and explosive applications that an attempt was made not only to understand its effects, but also to uncover

relationships between the parent molecular structure and decomposition, and to probe physicochemical processes. Because the temporal resolution of the interferometer and the spatial resolution of the IR beam precluded observation of differences in the gas product concentrations at pressure above 1000 psi, we conducted all studies of the effect of pressure on thermolysis with pressures in the 1-1000 psi range.

CATEGORY A1 : STRONG PRESSURE DEPENDENCE IN MOST PRODUCTS

X = NO₂
Y = ONO₂

RDX   DNNC   HMX   TNDBN   HNDZ   TNAZ

DNCP   TNSD   TNSU   CIS -1,3,5,7- TNAD   TRANS -1,3,5,7- TNAD   TRANS -1,4,5,8- TNAD

CH₃(NCH₂)₃NCH₃   HNCH₂CH₂NH   XCCH₂CH₂COOH   YCH₂CHCH₂CH₂Y   C(CH₂Y)₄
OHMX   EDNA   BTTN   PETN

CATEGORY A2 : STRONG PRESSURE DEPENDENCE IN ONLY ONE OR TWO PRODUCTS
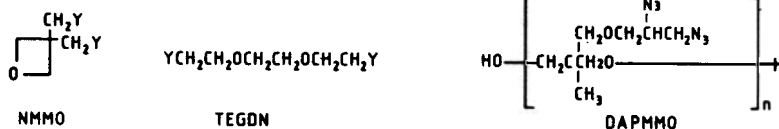
NMMO   TEGDN   DAPMMO

Figure 9. Selected compounds whose gas products display a strong pressure dependence in the 1-1000 psi range of *Ar*.

The categories of general behaviour emerge when the relative percentages of the first detected gas products from many of the compounds above are plotted against the applied *Ar* pressure[21]. A separate thermolysis experiment was performed at each pressure. Category A is shown in Fig. 9. It contains various nitramines, aliphatic nitro compounds and nitrate esters, and display a strong pressure dependence in all of the gas products. This category represents compounds that are found to release highly reactive gases, such as NO_2, and CH_2O, in the lower pressure range. Figure 10 illustrates this behaviour for DNCP. In the middle pressure range of 40-200 psi, a different set of products dominates. These products are those of intermediate stability, such as NO and HCN, and result, in part, from further reactions of the gases that dominate at lower pressure. At pressures above 200 psi, combustion-like products, CO, CO_2, H_2O and (probably) N_2 dominate because of still more extensive reaction

chemistry. It can be noted that *HONO* is not found at the lowest or highest pressures, but does appear in the mid pressure range. This is because NO_2 is released at low pressure and is not available to form *HONO*. As the pressure is raised, NO_2 remains in contact with the condensed phase for a longer period of time and produces *HONO* (vide supra). At the higher pressures, *HONO* decomposes before detection.
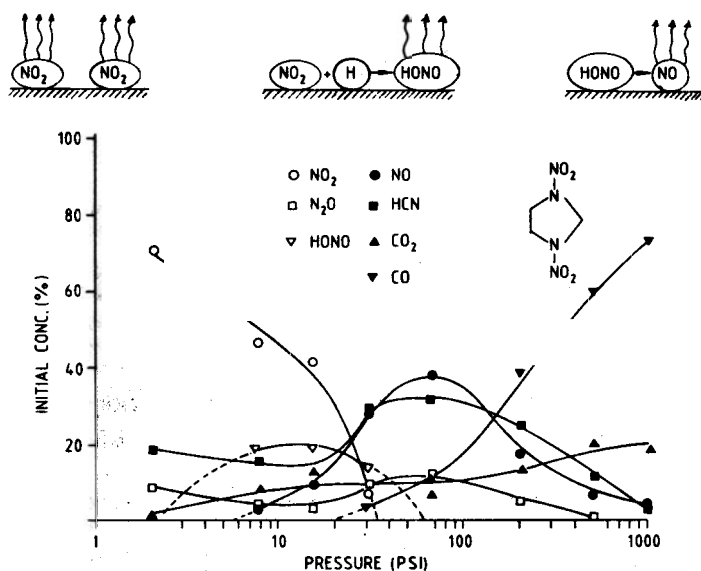

Figure 10.   Pressure dependence of the gas products from DNCP.

Category B shown in Fig. 11 contains compounds that produce gases exhibiting only a minor dependence on pressure[21]. As with the first category, more than one type of energetic functional group is represented: nitramines, aliphatic nitro compounds, and azides. Thus, the behaviour results from a general situation rather than the particular reaction mechanism of a functional group. Present are compounds that produce a reactive gas, such as NO_2, but that do not also liberate another product with which NO_2 can react. Also present are compounds that liberate relatively unreactive products initially, such as N_2 or N_2O, and compounds in which extensive condensed phase chemistry appears to have occurred before the gases reach the IR beam. Condensed phase chemistry is not especially pressure dependent. The source of the strong effect of pressure on the first category compounds has been demonstrated to result from the difference in the diffusion rates of the gases (and thus, their residence time with the condensed phase) as a function of the applied pressure[21]. The gases must percolate through the condensed phase. As the pressure is raised, the extent of heterogeneous gas phase/condensed phase reactions increases because the time of

percolation and residence increases. Thus, the yield of increasingly stable gas products increases with pressure. The three-zone behaviour shown in Fig. 10 simply reflects the natural progression in the nitrogen chemistry $[NO_2\,(HONO) \longrightarrow NO \longrightarrow N_2]$ and carbon chemistry $(CH_2O \longrightarrow CO, CO_2)$ toward the more thermodynamically stable products. There is no implication of a change in the decomposition mechanism as a function of pressure for these compounds in the 1-1000 psi range. It is interesting to note that this broad pattern of reaction behaviour resembles the theoretically derived[22] and experimentally measured[23,24] flame structure of nitramines as a function of distance from the surface.
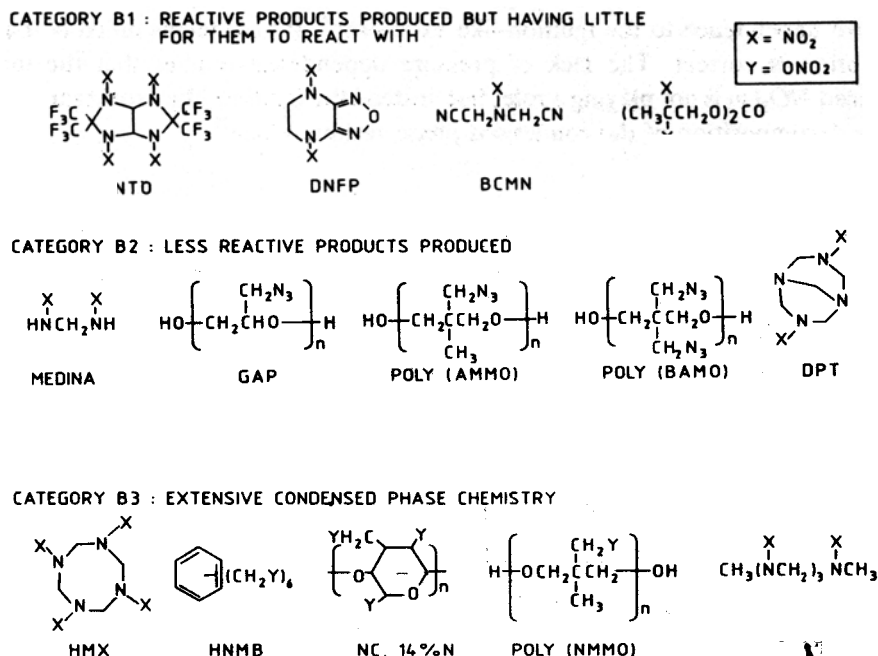

Figure 11. Selected compounds whose gas products are relatively independent of pressure in the 1-1000 psi range of *Ar*.

The above explanation for the source of the pressure dependence of the first-detected gases implies that initial pressure differences can be used to advantage. Fast thermolysis/FTIR data mostly reflect condensed phase processes[4]. In the temperature profiling/FTIR method, the temperature deflections caused by the condensed phase processes are measured simultaneously with the gas products[2]. Thus, the pressure dependence of the gas product distribution and the temperature deflection can be used to distinguish decomposition process involving the heterogeneous gas/condensed phase from those that are solely associated with the condensed phase.

The gas products and temperature deflections of alkylammonium nitrate salts are dependent on pressure[25]. Therefore, heterogeneous gas/condensed phase processes are important during their fast thermal decomposition. On the other hand, the temperature deflections of trinitromethyl compounds are mostly caused by reactions of the condensed phase alone without participation of the gas products[26]. This conclusion came about circuitously. These trinitromethylalkyl compounds are interesting from the standpoint of their tendency to produce NO_2 exclusively in an induction-like phase and then to transit sharply to an ignition-like or explosion phase. Figure 12 shows this behaviour for TEFO, $[(NO_2)_3 CCH_2]_2 CH_2$. This finding was first interpreted to originate from the $NO_2(g)$ initially produced returning to attack the hot condensed phase residue and igniting it[27,28]. However, because of the lack of a pressure dependence to the ignition-like exotherm[26], it now seems unlikely that this description is correct. The lack of pressure dependence implies that the initially produced $NO_2(g)$ is not playing a role, but, instead the ignition-like exotherm is caused by the decomposition of the condensed phase residue alone[26].

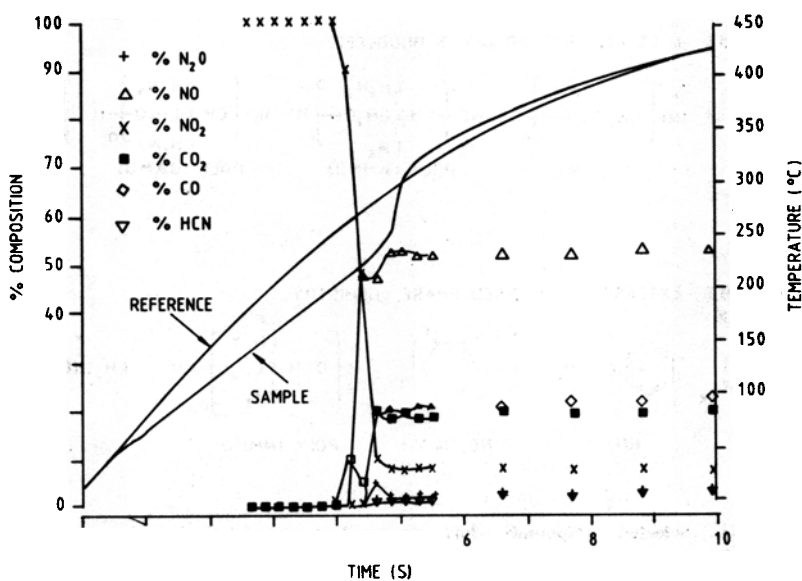Figure 12. Temperature profiling/FTIR spectroscopy of TEFO under 15 psi *Ar*.

REFERENCES

Oyumi, Y. & Brill, T.B. Thermal decomposition of energetic materials, 3: A high-rate *in situ*, FTIR of the thermolysis of RDX and HMX with pressure and heating rate as variables. *Combustion and Flame*, 1985, **62**, 213-24.

Cronin, J.T. & Brill, T.B. Thermal decomposition of energetic materials, 26: Simultaneous temperature measurements of the condensed phase and rapid-scan FTIR spectroscopy of the gas phase at high heating rate. *Applied Spectroscopy*, 1987, **41**, 1147-51.

3. Cronin, J.T. & Brill, T.B. Thermal decomposition of energetic materials, 33: The thermolysis pathway of the azidodinitromethyl group. *Applied Spectroscopy*, 1989, **43**, 650-53.

4. Palopoli, S.F. & Brill, T.B. Thermal decomposition of energetic materials, 51: On the foam zone and surface chemistry of rapidly decomposing HMX. *Combustion and Flame*, (submitted).

5. Brill, T.B. & Oyumi, Y. Thermal decomposition of energetic materials, 10: A relationship of molecular structure and vibrations to decomposition: polynitro-3, 3,7,7-tetrakis (trifluoromethyl)2,4,6,8-tetraazabicyclo[3.3.0] octanes, *J. Phys. Chem.*, 1986, **90**, 2679-83.

6. Oyumi, Y.; Rheingold, A.L. & Brill, T.B. Thermal decomposition of energetic materials, 18: Bis(cyanomethyl) nitramine and bis(cyanoethyl)nitramme. *Prop. Explos. Pyrotech.*, 1987, **12**, 1-7.

7. Brill, T.B. & Oyumi, Y. Thermal decomposition of energetic materials, 17: A relationship of molecular composition to *HONO* formation: bicyclo and spiro tetranitramines. *J. Phys. Chem.*, 1986, **90**, 6848-53.

8. Oyumi, Y. & Brill, T.B. Thermal decomposition of energetic materials, 21: The effect of backbone composition of the products evolved upon rapid thermolysis of linear nitramines. *Combustion and Flame*, 1987, **67**, 121-26.

9. Oyumi, Y. & Brill, T.B. Thermal decomposition of energetic materials, 25: Shifting of the dominant decomposition site by backbone substitution of alkylammonium nitrate salts. *J. Phys. Chem.*, 1987, **91**, 3657-61.

10. Oyumi, Y. & Brill, T.B. Thermal decomposition of energetic materials, 28: predictions and results for nitramines of bisimidazolidinedione, DINGU, TNGU and TDCD. *Prop. Explos. Pyrotech.*, 1988, **13**, 69-73.

Shaw, R. & Walker, F.E. Estimated kinetics and thermochemistry of some initial unimolecular reactions in the thermal decompostion 1,3,5-7-tetranitro-1,3,5, 7-tetraazacyclooctane in the gas phase. *J. Phys. Chem.*, 1977, **81**, 2572-76.

12   Fogel'zang, A.E.; Svetlov, B.S.; Adhemyan, V. Ya.; Kolyasov, S.M. & Sergienko, O.I. The combustion of nitramines and nitrosamines. *Doklady Akademii Nauk USSR*, 1974, **216**, 603-06.

Oyumi, Y. & Brill, T.B. Thermal decomposition of energetic materials, 4: High-rate *in situ*, thermolysis of four, six, and eight membered, oxygen-rich, *gem*-dinitroalkyl cyclic nitramines, TNAZ, DNNC and HNDZ. *Combustion and Flame*, 1985, **62**, 225-31.

14   Oyumi, Y. & Brill, T.B. Thermal decomposition of energetic materials, 11: Condensed phase structural characteristics and high rate thermolysis of di and trinitroaliphatic carboxylic acids and carbonates. *Combustion and Flame*, 1986, **65**, 103-11.

15. Gray, P. Bond dissociation energies in nitrites and nitro compounds and the reaction of free radicals with NO_2. *Trans. Farad. Soc.*, 1955, **51**, 1367-74.

16. Hoffsommer, J.C. & Glover, D.J. Thermal decomposition of 1,3,5-trinitro-1, 3,5-triazacyclohexane (RDX): kinetics and nitroso intermediates formation. *Combustion and Flame*, 1985, **59**, 303-10.

17   Behrens, R. Simultaneous thermogravimetric modulated beam mass spectroscopy and time-of-flight velocity spectra measurements: thermal decomposition mechanisms of RDX and HMX. *CPIA Publication*, 1987, **476**, Vol 1., 333-42.

Hoffsommer, J.C.; Glover, D.J. & Elban, W.L. Quantitative evidence for nitroso compound formation in drop-weight impacted RDX crystals. *J. Energy Materials*, 1985, **3**, 149-67.

19   Oyumi, Y. & Brill, T.B. Thermal decomposition of energetic materials, 5: High-rate *in situ*, thermolysis of two nitrosamine derivatives of RDX by FTIR spectroscopy. *Combustion and Flame*, 1985, **62**, 233-41.

20. Oyumi, Y.; Rheingold, A.L. & Brill, T.B. Thermal decomposition of energetic materials, 16: Solid-phase structural analysis and the thermolysis of 1,4-dinitrofurazano[3,4-b] piperazine. *J. Phys. Chem.*, 1986, **90**, 4686-90.

21   Oyumi, Y. & Brill, T.B. Thermal decomposition of energetic materials, 22: the contrasting effects of pressure on the high-rate thermolysis of 34 energetic compounds. *Combustion and Flame*, 1987, **68**, 209-16.

22. Melius, C.F. Molecular decomposition mechanisms of energetic materials. *J. Phys.*, 1987, **48**, C4-341-52.

23   Korobeinichev, O.P.; Kuibida, L.V.; Orlov, V.N.; Tereshchenko, A.G.; Kutsenogii, K.P.; Mavliev, R.A.; Ermolin, N.E.; Fomin, V.M. & Emel'yanov, I.D. Mass spectrometric probe study of the flame structure and kinetics of

chemical reactions in flames. *Mass Spect. and Chem. Kinetics*, 1985, 73-93.

24. Parr, T.P. & Hanson-Parr, D.M. The application of imaging laser induced fluorescence to the measurement of HMX and aluminized propellant ignition and deflagration flame structure. *CPIA Publication*, 1986, **457**, Vol. 1, 249-61.

25. Russell, T.P. & Brill, T.B. Thermal decomposition of energetic materials, 31: Fast thermolysis of ammonium nitrate, ethylenediamine dinitrate and hydrazinium nitrate and the relationship to the burning rate. *Combustion and Flame*, 1989, **76**, 393-401.

26. Brill, T.B. & Subramanian, R. Thermal decomposition of energetic materials, 35: A mechanism study of decomposition and the transition to the ignition-like state in trinitromethyl alkyl compounds. *Combustion and Flame*, 1990, **80**, 150-56.

27. Oyumi, Y.; Brill, T.B. & Rheingold, A.L. Thermal decomposition of energetic materials, 7: High-rate FTIR studies and the structural of 1,1,1,3,6,8,8, 8-octanitro-3,6-diazaoctane. *J. Phys. Chem.*, 1985, **89**, 4824-28.

28. Oyumi, Y. & Brill, T.B. Thermal decomposition of energetic materials, 15: Evidence that decomposition initiates deflagration: high-rate thermolysis of FEFO, TEFO & DITEFO. *Prop. Explos. Pyrotech.*, 1986, **11**, 35-39.